A LETTERS JOURNAL EXPLORING THE FRONTIERS OF PHYSICS

OFFPRINT

On the influence of dilute charged impurity and perpendicular electric field on the electronic phase of phosphorene: Band gap engineering

H. D. Bui, Le T. T. Phuong and Mohsen Yarmohammadi

EPL, **124** (2018) 27001

epl

A Letters Journal Exploring the Frontiers of Physics

AN INVITATION TO SUBMIT YOUR WORK

epljournal.org

The Editorial Board invites you to submit your Letters to EPL

Choose EPL, and you'll be published alongside original, innovative Letters in all areas of physics. The broad scope of the journal means your work will be read by researchers in a variety of fields; from condensed matter, to statistical physics, plasma and fusion sciences, astrophysics, and more.

Not only that, but your work will be accessible immediately in over 3,300 institutions worldwide. And thanks to EPL's green open access policy you can make it available to everyone on your institutional repository after just 12 months.

Run by active scientists, for scientists

Your work will be read by a member of our active and international Editorial Board, led by Bart Van Tiggelen. Plus, any profits made by EPL go back into the societies that own it, meaning your work will support outreach, education, and innovation in physics worldwide.

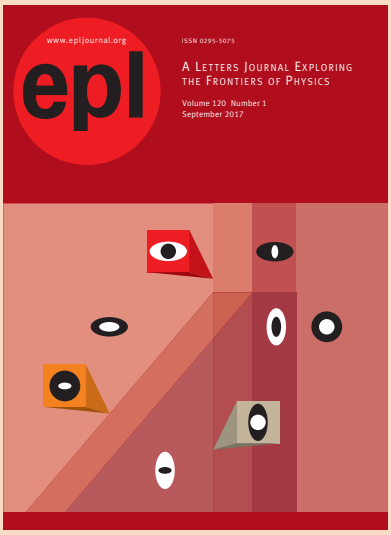

OVER

638,000

full-text downloads in 2017

Average submission to online publication

100 DAYS

21,500

citations in 2016

We greatly appreciate the efficient, professional and rapid processing of our paper by your team.

Cong Lin
Shanghai University

Four good reasons to publish with EPL

1. **International reach** – more than 3,300 institutions have access to EPL globally, enabling your work to be read by your peers in more than 90 countries.

2. **Exceptional peer review** – your paper will be handled by one of the 60+ co-editors, who are experts in their fields. They oversee the entire peer-review process, from selection of the referees to making all final acceptance decisions.

3. **Fast publication** – you will receive a quick and efficient service; the median time from submission to acceptance is 75 days, with an additional 20 days from acceptance to online publication.

4. **Green and gold open access** – your Letter in EPL will be published on a green open access basis. If you are required to publish using gold open access, we also offer this service for a one-off author payment. The Article Processing Charge (APC) is currently €1,400.

Details on preparing, submitting and tracking the progress of your manuscript from submission to acceptance are available on the EPL submission website, **epletters.net**.

If you would like further information about our author service or EPL in general, please visit **epljournal.org** or e-mail us at **info@epljournal.org**.

EPL is published in partnership with:

European Physical Society

Società Italiana di Fisica

EDP Sciences

IOP Publishing

A Letters Journal Exploring the Frontiers of Physics

October 2018

EPL, **124** (2018) 27001
doi: 10.1209/0295-5075/124/27001

www.epljournal.org

On the influence of dilute charged impurity and perpendicular electric field on the electronic phase of phosphorene: Band gap engineering

H. D. Bui[1], Le T. T. Phuong[2(a)] and Mohsen Yarmohammadi[3(b)]

[1] *Institute of Research and Development, Duy Tan University - 03 Quang Trung, Danang, Viet Nam*
[2] *Center for Theoretical and Computational Physics, University of Education, Hue University Hue City, Viet Nam*
[3] *Lehrstuhl für Theoretische Physik I, Technische Universität Dortmund - Otto-Hahn Straße 4, 44221 Dortmund, Germany*

received 21 September 2018; accepted in final form 17 October 2018
published online 13 November 2018

PACS 73.22.-f – Electronic structure of nanoscale materials and related systems
PACS 71.10.-w – Theories and models of many-electron systems
PACS 71.30.+h – Metal-insulator transitions and other electronic transitions

Abstract – Tuning the band gap plays an important role for applicability of 2D materials in the semiconductor industry. The present paper is a theoretical study on the band gap engineering using the electronic density of states (DOS) of phosphorene in the presence of dilute charged impurity and of a perpendicular electric field. The electronic DOS is numerically calculated using a combination of the continuum model Hamiltonian and the Green's function approach. Our findings show that the band gap of phosphorene in the absence and presence of the perpendicular electric field decreases with increasing impurity concentration and/or impurity scattering potential. Further, we found that in the presence of opposite perpendicular electric fields, the electronic DOS of disordered phosphorene shows different changing behaviors stemming from the Stark effect: in the positive case the band gap increases with increasing electric-field strength; whereas in the negative case the band gap disappears. The latter, in turn, leads to the semiconductor-to-semimetal and semiconductor-to-metal phase transition for the case of strong impurity concentrations and strong impurity scattering potentials, respectively. The results can serve as a base for future applications in logic electronic devices.

Introduction. – Graphene [1–4], a honeycomb structured two-dimensional (2D) material, offers intriguing potential applications in next-generation electronic devices [5–8]. From the intensive research interests on graphene after the wake of 2004, a broad research enthusiasm on other 2D materials has been ignited. Like carbon, phosphorus also possesses a 2D honeycomb structure, the so-called monolayer black phosphorus (MBP), phosphorus (P) analog of graphene [9]. MBP has a puckered structure in which sp^3 hybridized P atoms are held together mostly by weak van der Waals forces [10]. Also, there is an anisotropic in MBP structure due to the different carrier effective masses along the zigzag and armchair directions. Anisotropic electronic transport and optical properties of MBP are also reported in experimental studies [11,12].

The direct band gap in all forms of MBP from the monolayer to bulk distinguishes it from other 2D materials [13]. For instance, gapless graphene is a semi-metal and transition-metal dichalcogenides (TMDs) illustrate a direct band gap just in monolayer form [14–16]. A band gap plays an important role in the fabrication of electronic devices, especially semiconductor devices like the field effect transistors (FETs). Lack of the band gap limits the application of graphene in the industry [17] and on the other hand, a large direct band gap in TMDs also restricts the application of TMDs in high ON/OFF current ratio [18]. Recent researches have shown that MBP with a moderate band gap has the potential to be a good candidate for semiconducting technology [19]. Further,

(a) E-mail: thuphuonghueuni@gmail.com
(b) E-mail: mohsen.yarmohammadi@tu-dortmund.de

the integer quantum Hall effect in high-quality black phosphorus 2D electron systems with the carrier Hall mobility up to 6000 $\mathrm{cm}^2\ \mathrm{V}^{-1}\ \mathrm{s}^1$ has been reported in ref. [20], in which the results are useful for further study on quantum transport and device application of MBP in the ultrahigh mobility regime.

Obviously, optimizing electronic features of MBP requires to control the electronic phases. Further, there are several methods to make the band gap tunable such as applying an electric field, strain [21,22], and defects [23,24]. This work is aimed at implementing and demonstrating a theoretical framework that shows an electronic phase transition in dilute charged impurity-infected MBP. There are two basic types of scattering mechanisms that influence the mobility of electrons, lattice scattering, and impurity scattering. At low temperatures, carriers move more slowly, so they have more time to interact with impurities. Accordingly, the impurity scattering increases with decreasing temperature, leading to the reduction of mobility. This is just the opposite of the effect of lattice scattering because lattice vibrations cause the mobility to decrease with increasing temperature [25]. Here we are interested in the impurity scattering. Impurity effects on the properties of devices could be introduced by many quantities, but the electronic density of states (DOS) is the best character to study the behavior of carriers in the presence of an impurity. From this quantity, other electronic and optical properties of the material would be understood easily.

For the sake of conciseness, we concentrate our discussion on the implementation of Born approximation in the electronic-structure of disordered MBP. However, the proposed methodology is applicable in a straightforward fashion also in *ab initio* codes and in different electronic-structure methods. The overall goal of this paper is to elucidate, discuss, and explain the electronic phase transition in dilute charged impurity-infected biased MBP. The perpendicular electric field introduces by the bias gate voltage. Accordingly, the remainder of this manuscript is organized as follows: In the second section, the required theoretical framework used in state-of-the-art Green's function technique is introduced. In particular, we discuss how one calculates the non-interacting and interacting Green's functions. In the third section, we then discuss possible phase transitions and required conditions that we envision to implement and use during this research. In the last part of this paper (the fourth section), we summarize our main conclusions.

Theory and method. –

Model description and non-interacting Green's function. Let us now consider the case of MBP with an orthorhombic crystal structure, emphasizing the in-plane translational symmetry. The top view of the real space of MBP with P atoms in the upper and lower sublayers are represented by red and black circles in fig. 1(a). To proceed, we take into account the C_{2h} group

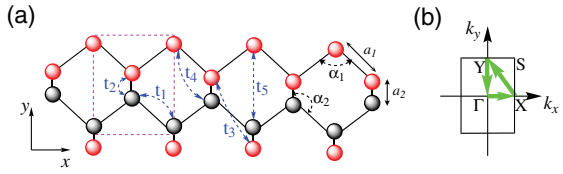

Fig. 1: (Color online) (a) Top view geometry of MBP. Each unit cell (the pink rectangle) consists of four atoms, as illustrated by red and black circles. The first Brillouin zone of MBP is illustrated in (b) with high-symmetry points Γ, X, S, and Y.

invariance-included [26] tight-binding model proposed in ref. [27] as

$$\mathcal{H}(\mathbf{k}) = \begin{pmatrix} t_{AD}(\mathbf{k}) & t_{AB}(\mathbf{k}) + t_{AC}(\mathbf{k}) \\ [t_{AB}(\mathbf{k}) + t_{AC}(\mathbf{k})]^* & t_{AD}(\mathbf{k}) \end{pmatrix}, \quad (1)$$

with structure factors given by

$$t_{AB}(\mathbf{k}) = 2t_1 \cos[k_x a_1 \sin(\alpha_1/2)] e^{-\mathrm{i}k_y a_1 \cos(\alpha_1/2)} + 2t_3 \cos[k_x a_1 \sin(\alpha_1/2)] e^{\mathrm{i}k_y [a_1 \cos(\alpha_1/2) + 2a_2 \cos(\beta)]}, \quad (2a)$$

$$t_{AC}(\mathbf{k}) = t_2 e^{\mathrm{i}k_y a_2 \cos(\beta)} + t_5 e^{-\mathrm{i}k_y [2a_1 \cos(\alpha_1/2) + a_2 \cos(\beta)]}, \quad (2b)$$

$$t_{AD}(\mathbf{k}) = 4t_4 \cos[k_x a_1 \sin(\alpha_1/2)] \times \cos(k_y [a_1 \cos(\alpha_1/2) + a_2 \cos(\beta)]), \quad (2c)$$

where $a_1 = 2.22\,\text{Å}$ is the distance between nearest-neighbor P atoms in each sublayer with the hopping parameter t_1 and $a_2 = 2.24\,\text{Å}$ is the distance between one P atom in upper (lower) sublayer with the nearest-neighbor atom in the lower (upper) sublayer with the hopping parameter t_2. The bond angles are also given by $\alpha_1 = 96.5°$, $\alpha_2 = 101.9°$ and $\cos(\beta) = -\cos(\alpha_2)/\cos(\alpha_1)$. The hopping parameters taken from ref. [27] are listed in table 1. Using the expanded tight-binding model proposed by Rodin *et al.* [28] around the Γ-point and retaining the terms up to second-order in momentum, the continuum approximation of the MBP model Hamiltonian would be achieved as [28]

$$\mathcal{H}(\mathbf{k}) = \begin{pmatrix} \epsilon_\mathrm{c} + \eta_\mathrm{c} k_x^2 + \nu_\mathrm{c} k_y^2 & \gamma k_x + \alpha k_x^2 + \beta k_y^2 \\ \gamma k_x + \alpha k_x^2 + \beta k_y^2 & \epsilon_\mathrm{v} - \eta_\mathrm{v} k_x^2 - \nu_\mathrm{v} k_y^2 \end{pmatrix}, \quad (3)$$

which is in the basis of envelope wave functions associated with the probability amplitude at the respective sublattice sites. In the equation above, $\epsilon_\mathrm{c} = 2t_1 + t_2 + 2t_3 + 4t_4 + t_5$ and $\epsilon_\mathrm{v} = -(2t_1 + t_2 + 2t_3 - 4t_4 + t_5)$ are the energies from the bottom of the conduction band and the top of the valence band at the Γ-point, respectively, making a direct energy gap $\mathcal{E}_g = 1.52\,\text{eV}$ in agreement with refs. [26,29]. $\mathbf{k} = (k_x, k_y)$ stands for the momenta belonging to the first Brillouin zone (FBZ). On the basis of DFT calculations [30], other coefficients in eq. (3) are $\eta_\mathrm{c} = 0.008187$, $\eta_\mathrm{v} = 0.038068$, $\nu_\mathrm{c} = 0.030726$, $\nu_\mathrm{v} = 0.004849$ in units of eVnm^2, and $\gamma = 0.48$ in unit of eVnm. By considering $\alpha \ll \gamma$ and time-reversal invariant (TRI) in the system,

Table 1: The hopping parameters taken from ref. [27].

Parameter	Value (eV)
t_1	-1.220
t_2	$+3.665$
t_3	-0.205
t_4	-0.105
t_5	-0.055

one might delete terms including α and β and the new Hamiltonian by considering V as variable gate voltage can be rewritten as

$$\mathcal{H}(\mathbf{k}) = \begin{pmatrix} \mathcal{H}_{\rm c} & \mathcal{H}_{\rm cv} \\ \mathcal{H}_{\rm cv} & \mathcal{H}_{\rm v} \end{pmatrix}, \tag{4}$$

where

$$\mathcal{H}_{\rm c} = \epsilon_{\rm c} + \eta_{\rm c} k_x^2 + \nu_{\rm c} k_y^2 - V/2, \tag{5a}$$

$$\mathcal{H}_{\rm v} = \epsilon_{\rm v} - \eta_{\rm v} k_x^2 - \nu_{\rm v} k_y^2 + V/2, \tag{5b}$$

$$\mathcal{H}_{\rm cv} = \gamma k_x, \tag{5c}$$

where $V = eEd$ is the applied bias voltage referring to the electric field E, the elementary charge e, and the sublayer separation d. By diagonalizing the Hamiltonian above, one obtains the following energy dispersion relation for electrons ($\tau = +1$) and holes ($\tau = -1$):

$$\mathcal{E}_\tau = \frac{1}{2}\Big[\mathcal{H}_{\rm c} + \mathcal{H}_{\rm v} + \tau\sqrt{4\mathcal{H}_{\rm cv}^2 + (\mathcal{H}_{\rm c} - \mathcal{H}_{\rm v})^2}\Big]. \tag{6}$$

On account of the fact that several studies have been carried out the band structure of MBP using different approaches [31–33], we use DOS of MBP in order to discuss the main features of our results. By the end of the analytical studying the properties of MBP, we have employed the non-interacting and interacting Green's function technique within the Born approximation in the scattering theory. Since the unit cell of MBP contains four atoms, the Green's function can be written as a 4×4 matrix, but using TRI and $G_0(\mathbf{k}, \mathcal{E}) = [\mathcal{E} + \mathtt{i}\zeta - \mathcal{H}(\mathbf{k})]^{-1}$ for $\zeta = 5\,\text{meV}$, we deduce the following non-interacting Green's function matrix in the momentum space:

$$G_0(\mathbf{k}, \mathcal{E}) = \begin{pmatrix} \mathcal{E} + \mathtt{i}\zeta - \mathcal{H}_{\rm c} & -\mathcal{H}_{\rm cv} \\ -\mathcal{H}_{\rm cv} & \mathcal{E} + \mathtt{i}\zeta - \mathcal{H}_{\rm v} \end{pmatrix}^{-1} = \begin{pmatrix} G_0^{\rm c}(\mathbf{k}, \mathcal{E}) & G_0^{\rm cv}(\mathbf{k}, \mathcal{E}) \\ G_0^{\rm cv}(\mathbf{k}, \mathcal{E}) & G_0^{\rm v}(\mathbf{k}, \mathcal{E}) \end{pmatrix}. \tag{7}$$

Using the solution of $G_0(\mathbf{k}, \mathcal{E})$ and the Born approximation, DOS, in order to study the electronic phase transition in MBP, can be expressed.

Interacting Green's function. Throughout this section, the dilute charged impurities characterized by impurity concentration n_i and scattering potential ν_i have been added to the system randomly aimed at controlling the band gap. The interaction between the electrons of MBP and dilute charged impurities using the tight-binding model is given by

$$\mathcal{H}_{\text{e-i}} = \sum_{\mathbf{q}} \nu_{\rm i} c_{\mathbf{q}}^\dagger c_{\mathbf{q}}, \quad c = \{\text{unit cell atoms}\}, \tag{8}$$

where the momenta $\mathbf{q}$ induced by impurities to the host electrons belong to the FBZ. According to the Born approximation in the scattering theory and using the T-matrix [34,35], the electronic self-energy matrix elements of disordered MBP can be obtained by

$$\Sigma(\mathbf{q}, \mathcal{E}) = n_i \nu_i \bigg(1 - \frac{\nu_i}{N_i} \sum_{\mathbf{k} \in \text{FBZ}} G_0(\mathbf{k}, \mathcal{E})\bigg)^{-1}, \tag{9}$$

where N_i is the number of impurity atoms per unit cell. Full self-consistent Born approximation originates from the expression of the self-energy matrix in eq. (9). It is worth mentioning that although we use the Born approximation, *i.e.*, small density of impurities, the Friedel charge oscillation exists [36] and oscillates in BP anisotropically in the x and y directions. However, investigation of the Friedel charge oscillation is outside of the scope of the present paper and perhaps we will focus on that in our future works. The perturbed configuration of Green's function through the Dyson equation [34] reads

$$G(\mathbf{k}, \mathcal{E}) = \frac{G_0(\mathbf{k}, \mathcal{E})}{1 - \Sigma(\mathbf{q}, \mathcal{E}) G_0(\mathbf{k}, \mathcal{E})}. \tag{10}$$

Evidently, DOS can be related to the trace over the imaginary part of retarded Green's function

$$\mathcal{D}(\mathcal{E}) = -\frac{1}{\pi N_a N_c} \sum_{\alpha = \text{c, v}} \sum_{\mathbf{k} \in \text{FBZ}} \Im G^\alpha(\mathbf{k}, \mathcal{E}), \tag{11}$$

where N_a and N_c are the number of atoms per unit cell and the number of unit cells, respectively. Due to the randomness nature of impurities, we have considered 1000×1000 configurations in the numerical calculations of the electronic DOS of disordered phosphorene and finally, the result of the electronic DOS is then obtained by making an average over these configurations. The impurity concentration considered in the present work reaches up to 20%. Such a high concentration is clearly true for the case of *dilute* charged impurities as assumed in the theoretical model because $n_i = x\%$ in our numerical calculations means that $x\%$ of the whole 1000×1000 unit cells are infected by impurities and for this huge unit cell, 20% is still dilute. For the purpose of studying the electronic phase transition by using the phase desegregation in the MBP system, we use DOS in the vicinity of Fermi energy. We would like to stress that Fermi energy is set to zero as well as the structure of the system is in its stable (optimized) state in the absence and presence of impurities.

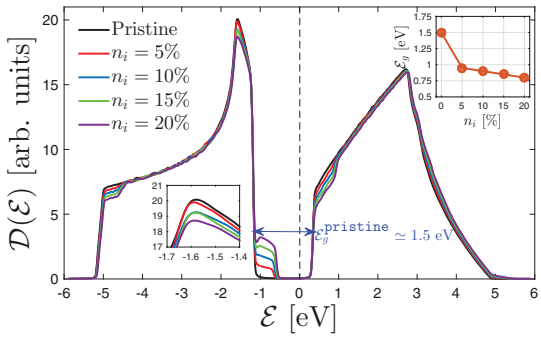

Fig. 2: (Color online) The electronic DOS of pristine and dilute charged impurity-induced MBP with impurity concentration n_i at a constant scattering potential $\nu_i = 0.5\,\text{eV}$ in the absence of a perpendicular electric field. The evaluation of the van Hove singularity of the valence band and the band gap with n_i are shown in the inset panels.

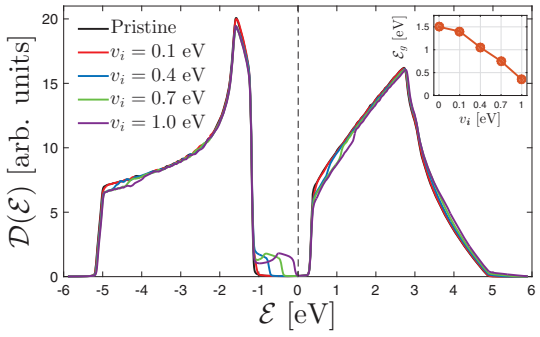

Fig. 3: (Color online) DOS of unbiased dilute charged impurity-induced MBP as the scattering potential ν_i is changed. The impurity concentration is fixed at $n_i = 10\%$. Dependence of the band gap energy $\mathcal{E}_g$ on ν_i is presented in the inset panel.

Concluding remarks. – An analysis of the main findings is presented in this section. We numerically study the effect of dilute charge impurity and the perpendicular electric field on the electronic DOS of MBP as a function of energy in the range from $-6\,\text{eV}$ to $+6\,\text{eV}$. This section is divided into two parts. In the first part, we investigate the effect of impurity on DOS (figs. 2, 3, and 4) and the second part analyses the effect of opposite perpendicular electric fields on DOS of impurity-infected MBP in fig. 5.

As is well known in the literature, there is a strong anisotropy property in dispersion energy of MBP due to the direction-dependent effective mass and Fermi velocity of carriers [37,38]. It has been reported that the velocity of a hole or an electron along the x-direction takes a higher value than in the y-direction for the conduction band, whilst the valence band behaves inversely [37]. Because of this, the effective mass at the Γ-point is heaver along the y-direction than along the x-direction. Anisotropic features of MBP make it more applicable for optoelectronics devices [39]. Here, we show the total DOS by summing over the whole FBZ not by taking the average over different directions. It means that in our numerical calculations, for each k_x within the range from $-\pi/l_x$ to $+\pi/l_x$, k_y changes from $-\pi/l_y$ to $+\pi/l_y$, where $l_x = 2a_1 \sin(\alpha/2)$ and $l_y = 2[a_1 \cos(\alpha/2) + a_2 \cos(\beta)]$ are the lattice parameters in the x- and y-direction, respectively [40]. The shape of DOS plotted here is in good agreement with ref. [41]. The band gap obtained in the present work and also refs. [26,27,42–44] is about 1.5 eV. We separate the electronic phases based on the rule: DOS at Fermi level is zero and non-zero for insulator/semiconductor and metal/semimetal materials.

Impurity effects. In the first part, we asses the electronic DOS of MBP in the presence of dilute charged impurities when the perpendicular electric field characterized by bias voltage V is absent and/or present. It should be noted that the impurity concentration n_i changes at a constant scattering potential ν_i and inversely. It is necessary to mention that based on the Born approximation, different n_i refers to *the same* impurity atoms, whilst different ν_i stands for *different* ones. As such, in order to evaluate the influence of impurity concentration on the electronic phase of MBP, we have plotted perturbed DOS with different percentages of n_i at impurity scattering potential $\nu_i = 0.5\,\text{eV}$. Also, we would like to stress again that we have focused on the perturbed DOS at the Fermi level $\mathcal{E} = 0$ in order to investigate the electronic phase of MBP. As can be seen from fig. 2, some *midgap* states emerge in the perturbed DOS, correspondingly the band gap of unbiased MBP decreases as n_i is increased. It is bearing in mind that within the Born approximation, *i.e.*, dealing with the finite but small density of impurities, peaks can show up in the DOS. Since they appear inside the band gap, the states associated with these peaks are called midgap states. These midgap states can be viewed as bound states attracted by the impurity potential. For many impurities with a small density, midgap states are related to the poles of self-energy function (T-matrix). On the other hand, we know from eq. (11) that the DOS is related to poles of Green's function. Thus, midgap states stem from new poles associated with impurity. The midgap states prepare the ground for tuning the band gap of MBP, as a result of this, usage of MBP gets up in the electronic applications. In addition, fig. 2 clearly shows that the value of the valence van Hove singularity decreases with n_i (the inset bottom left panel), meaning that the degeneracy level of the states at $\mathcal{E} = -1.6\,\text{eV}$ is broken and/or reduced. The band gap $\mathcal{E}_g$ as a function of the impurity concentration is shown in the inset in the top right panel, which illustrates that an increase in n_i causes a decrease in the band gap.

Further, we try to study the effect of the impurity scattering potential on the electronic DOS of unbiased MBP. So to achieve the best results we investigate disordered DOS of MBP with different values of ν_i at fixed impurity concentration equal to 10%. From fig. 3 it can be found

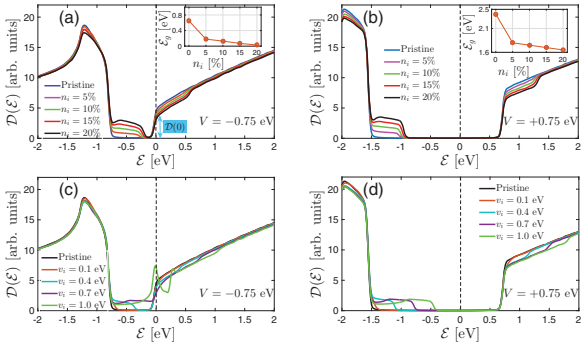

Fig. 4: (Color online) The electronic DOS of MBP for different impurity concentrations in the presence of gate voltage fixed at (a) $-0.75\,\mathrm{eV}$ and (b) $+0.75\,\mathrm{eV}$. Also, in panels (c) and (d) corresponding to $V = -0.75\,\mathrm{eV}$ and $V = +0.75\,\mathrm{eV}$, respectively, the perturbed DOS for different ν_i are presented.

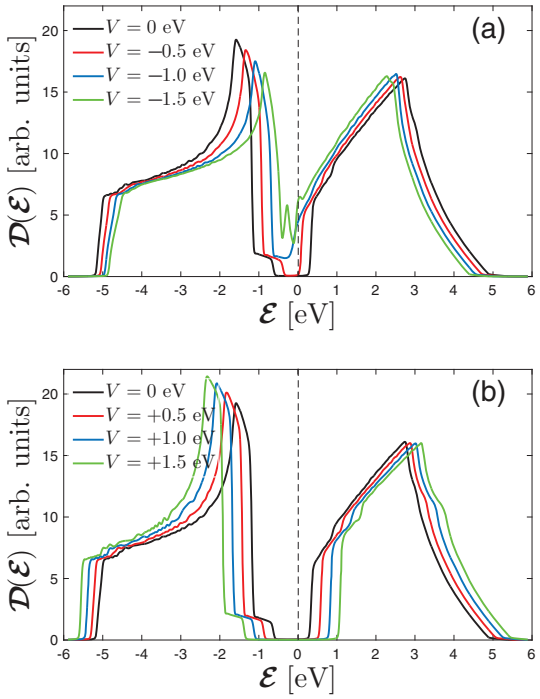

Fig. 5: (Color online) DOS of impurity-infected MBP with $n_i = 10\%$ and $\nu_i = 0.5\,\mathrm{eV}$ in the presence of (a) negative and (b) positive gate voltage.

that thanks to the emergence of the midgap states in the presence of dilute charged impurity, the band gap of MBP reduces by increasing the impurity scattering potential as well to the extent that most probably no band gap is observed at $\nu_i > 1\,\mathrm{eV}$. Our findings are in good agreement with first-principles calculations findings for which it has been shown that the various types of point defects lead to the appearance of the similar midgap states in DOS of MBP [23,45]. Thus, the overlapped impurity states in the valence and conduction bands in strong impurity scattering potential, which is not within the limit of the Born approximation, lead to a *semiconductor-to-semimetal* phase transition in MBP.

The main difference between the case of different n_i and different ν_i corresponding to the same impurity sources and different impurity sources refers to the value of the reduced band gap, where for the case of different ν_i, the decreasing trend is severely much sharper than the case of different n_i. From the results of the electronic DOS in the presence of dilute charged impurities, it can be inferred that charged impurities give rise to no resonant peaks in the DOS. However, it has been shown both experimentally [46] and theoretically [47] that native atomic vacancies (*i.e.*, phosphorus vacancies) can induce resonant states within the band gap of the phosphorene systems.

Now let us study disordered MBP in the presence of a constant perpendicular electric field for opposite poles of the applied gate. When applying a perpendicular electric field to phosphorene, it has been shown that the intralayer charge screening can be induced in phosphorene due to its puckered lattice structure (two sublayers). The field-induced charge screening plays a significant role in tuning the electronic properties (such as the band gap) of phosphorene and its multilayers [48]. However, we have ignored the effect of intralayer charge screening in the present work. Panels (a) and (b) in fig. 4 represent the perturbed DOS by *the same* impurity atoms (different n_i) of biased MBP with the bias voltage $V = -0.75\,\mathrm{eV}$ and $V = +0.75\,\mathrm{eV}$, respectively. As can be clearly seen, the band gap of the pristine MBP decreases (increases) with the negative (positive) case of the perpendicular electric field in good agreement with ref. [49]. The negative value of the perpendicular electric field means that we have switched the poles of the applied gate to the sublayers. However, similarly to the previous cases, the values of the decreased (increased) band gap decreases further in the presence of dilute charged impurity for the negative (positive) case of the perpendicular electric field, as shown in the insets in the top right panels, leading to the semiconductor-to-semimetal phase transition in the case of $V = -0.75\,\mathrm{eV}$ because of the non-zero value of DOS at the Fermi energy, *i.e.*, $\mathcal{D}(0)$.

Additionally, in panels (c) and (d), perturbed DOS by the *different* impurity atoms (different ν_i) for both $V = -0.75\,\mathrm{eV}$ and $V = +0.75\,\mathrm{eV}$ are studied, respectively. Obviously, the band gap decreases as ν_i is increased in both cases, leading to the semiconductor-to-metal phase transition in the case of $V = -0.75\,\mathrm{eV}$ because the non-zero value of DOS in (c) is much higher than (a), while in the case of $V = +0.75\,\mathrm{eV}$, the band gap only decreases with ν_i. A decrease in the band gap at strong impurity scattering potentials is more than the corresponding value of $\mathcal{E}_g$ for strong impurity concentrations. Consequently, by applying the electric field, in addition to the decrease of the band gap, a semiconductor-to-semimetal (metal) phase transition occurs at strong impurity concentrations (scattering potentials). The physical reasons for these effects will be discussed more in the next part.

Perpendicular electric-field effects. From fig. 4, we noticed that the layout of the gates is important. For the purpose of investigation of the impacts of the perpendicular electric field on the electronic properties of MBP, the disordered electric field-dependent DOS of MBP with $V < 0$ and $V > 0$ are depicted in fig. 5(a) and (b), respectively. In recent years there has been growing interest in the investigation of the effects of an electric field on the electronic dispersion of 2D materials [44,50,51]. As was stated already, MBP has two sublayers, therefore, applying gate potential leads to different on-site potentials $\pm V/2$ in the top and bottom sublayers of MBP, respectively. As expected, in the presence of negative (positive) gate voltage there is a decrease (an increase) in the band gap because, from the intuitive thoughts, the electronic DOS of disordered phosphorene should exhibit a symmetric behavior in the presence of opposite perpendicular electric fields. This is in agreement with previous results reported in the literature [49,50]. Interestingly, we found that the disordered DOS of biased MBP in the presence of impurity doping with $n_i = 10\%$ and $\nu_i = 0.5\,\mathrm{eV}$ showcases a semiconductor-to-metal phase transition in the presence of negative gate potential. Figure 5(b) reveals that there is no phase transition as long as the value of the gate voltage is positive.

As can be seen, the pair of van Hove singularities approaches the Fermi level $\mathcal{E} = 0\,\mathrm{eV}$ for $V < 0$, leading to the decrease of the degeneracy strength in the valence band, whereas in the case of $V > 0$, van Hove singularities get away from the Fermi level, resulting in the increase of the degeneracy strength in the valence band. These behaviors stem from our model in eq. (5), in which for $V < 0$ ($V > 0$), the energy dispersion of valence electrons decreases (increases). From the quantum-physical point of view, in the valence and conduction bands close to the Fermi level, new allowed energy levels emerge originating from the Stark effect when applying the electric field. On the other hand, in the presence of impurity, the impurity distribution resulting in midgap states plays a vital role in determining the final state of carriers. The competition between the impurity distribution and applied electric field leads to the asymmetric Stark effect and eventually the inversion symmetry breaks down [52,53]. In turn, the spatial distribution of electronic waves is broadened in the case of $V > 0$ because of the existence of more options for bounding. Whilst when switching the poles of the applied gate, the inverse Stark effect occurs and the electronic waves overlap efficiently.

Conclusions. – In this letter, we have attempted to assess the effects of dilute charged impurity and perpendicular electric field (bias potential) on the electronic DOS of MBP using the Green's function technique, Born approximation, and the continuum approximation of the tight-binding model. The results of this investigation show that the perturbed DOS indicates some midgap states in comparison with pristine in the presence of the dilute charged impurity. Accordingly, the band gap of impurity-induced MBP is less than the pristine one. Interestingly, we found that impurity-infected MBP shows semimetallic (metallic) behavior at strong impurity concentrations (scattering potentials), whereas pristine MBP is a semiconductor. Therefore, tuning the band gap of MBP makes it more applicable in electro-optical devices. Further, The results of applying the gate potential reveal that the band gap of MBP increases (decreases) in the presence of positive (negative) gate potential due to the Stark effect and surprisingly, the semiconductor-to-metallic phase transition emerges for the negative gate voltage.

* * *

This research is funded by Vietnam National Foundation for Science and Technology Development (NAFOSTED) under grant No. 103.01-2016.83.

REFERENCES

[1] Novoselov K. S., Geim A. K., Morozov S. V., Jiang D., Zhang Y., Dubonos S. V., Grigorieva I. V. and Firsov A. A., *Science*, **306** (2004) 666.
[2] Novoselov K. S., Geim A. K., Morozov S. V., Jiang D., Katsnelson M. I., Grigorieva I. V., Dubonos S. V. and Firsov A. A., *Nature*, **438** (2005) 197.
[3] Zhang Y., Tan Y.-W., Stormer H. L. and Kim P., *Nature*, **438** (2005) 201.
[4] Tang Q., Zhou Z. and Chen Z., *Nanoscale*, **5** (2013) 4541.
[5] Berger C., Song Z., Li X., Wu X., Brown N., Naud C., Mayou D., Li T., Hass J., Marchenkov A. N., Conrad E. H., First P. N. and de Heer W. A., *Science*, **312** (2006) 1191.
[6] Novoselov K. S., Jiang Z., Zhang Y., Morozov S. V., Stormer H. L., Zeitler U., Maan J. C., Boebinger G. S., Kim P. and Geim A. K., *Science*, **315** (2007) 1379.
[7] Tombros N., Jozsa C., Popinciuc M., Jonkman H. T. and van Wees B. J., *Nature*, **448** (2007) 571.
[8] Ohta T., Bostwick A., Seyller T., Horn K. and Rotenberg E., *Science*, **313** (2006) 951.
[9] Li L., Yu Y., Ye G. J., Ge Q., Ou X., Wu H., Feng D., Chen X. H. and Zhang Y., *Nat. Nanotechnol.*, **9** (2014) 372.
[10] Shulenburger L., Baczewski A. D., Zhu Z., Guan J. and Tomanek D., *Nano Lett.*, **15** (2015) 8170.
[11] Mao N., Tang J., Xie L., Wu J., Han B., Lin J., Deng S., Ji W., Xu H., Liu K., Tong L. and Zhang J., *J. Am. Chem. Soc.*, **138** (2015) 300.
[12] Cakir Deniz, Sevik Cem and Peeters François M., *Phys. Rev. B*, **92** (2015) 165406.
[13] Zhang S., Yang J., Xu R., Wang F., Li W., Ghufran M., Zhang Y. W., Yu Z., Zhang G., Qin Q. and Lu Y., *ACS Nano*, **8** (2014) 9590.
[14] Geim A. K. and Novoselov K. S., *Nat. Mater.*, **6** (2007) 183.

[15] Mak K. F., Lee C., Hone J., Shan J. and Heinz T. F., *Phys. Rev. Lett.*, **105** (2010) 136805.

[16] Yang J., Lu T., Myint Y. W., Pei J., Macdonald D., Zheng J. C. and Lu Y., *ACS Nano*, **9** (2015) 6603.

[17] Castro Neto A. H., Guinea F., Peres N. M. R., Novoselov K. S. and Geim A. K., *Rev. Mod. Phys.*, **81** (2009) 109.

[18] Ryou J., Kim Y.-S., KC S. and Cho K., *Sci. Rep.*, **6** (2016) 29184.

[19] Liu H., Neal A. T., Zhu Z., Luo Z., Xu X., Tomanek D. and Ye P. D., *ACS Nano*, **8** (2014) 4033.

[20] Li L., *et al.*, *Nat. Nanotechnol.*, **11** (2016) 593.

[21] Guo H., Lu N., Dai J., Wu X. and Zeng X. C., *J. Phys. Chem. C*, **118** (2014) 14051.

[22] Appalakondaiah S., Vaitheeswaran G., Lebegue S., Christensen N. E. and Svane A., *Phys. Rev. B*, **86** (2012) 035105.

[23] Ziletti A., Carvalho A., Campbell D. K., Coker D. F. and Castro Neto A. H., *Phys. Rev. Lett.*, **114** (2015) 046801.

[24] Wang G., Pandey R. and Karna S. P., *Appl. Phys. Lett.*, **106** (2015) 173104.

[25] Ashcroft N. and Mermin N., *Solid State Physics*, HRW international editions (Holt, Rinehart and Winston) 1976.

[26] Esawa M., *New J. Phys.*, **16** (2014) 115004.

[27] Rudenko A. N. and Katsnelson M. I., *Phys. Rev. B*, **89** (2014) 201408(R).

[28] Rodin A. S., Carvalho A. and Castro Neto A. H., *Phys. Rev. Lett.*, **112** (2014) 176801.

[29] Zhang R., *et al.*, *2D Mater.*, **2** (2015) 045012.

[30] Elahi M., Khaliji K., Tabatabaei S. M., Pourfath M. and Asgari R., *Phys. Rev. B*, **91** (2015) 115412.

[31] Allec S. I. and Wong B. M., *J. Phys. Chem. Lett.*, **7** (2016) 4340.

[32] Cupo A. and Meunier V., *J. Phys.: Condens. Matter*, **29** (2017) 283001.

[33] Zhou J. Z. S. and Liu N., *Comput. Mater. Sci.*, **130** (2017) 56.

[34] Mahan G. D., *Many Particle Physics* (Plenum Press, New York) 1993.

[35] Grosso G. and Parravicini G. P., *Solid State Physics,* 2nd edition (Academic Press, New York) 2014.

[36] Zou Y.-L., *et al.*, *Phys. Rev. B*, **94** (2016) 035431.

[37] Yuan S., Rudenko A. N. and Katsnelson M. I., *Phys. Rev. B*, **91** (2015) 115436.

[38] Rudenko A. N., Yuan S. and Katsnelson M. I., *Phys. Rev. B*, **92** (2015) 085419.

[39] Xia F., Wang H., and Jia Y., *Nat. Commun.*, **5** (2014) 4458.

[40] de Sousa D. J. P., de Castro L. V., da Costa D. R., Pereira J. Milton jr. and Low Tony, *Phys. Rev. B*, **96** (2017) 155427.

[41] Zare M., Parhizgar F. and Asgari R., *J. Magn. & Magn. Mater.*, **456** (2018) 307.

[42] de Sousa D. J. P., de Castro L. V., da Costa D. R. and Pereira J. Milton jr., *Phys. Rev. B*, **94** (2016) 235415.

[43] Zhou X. Y., Zhang R., Sun J. P., Zou Y. L., Zhang D., Lou W. K., Cheng F., Zhou G. H., Zhai F. and Kai Chang, *Sci. Rep.*, **5** (2015) 12295.

[44] Pereira J. M. jr. and Katsnelson M. I., *Phys. Rev. B*, **92** (2015) 075437.

[45] Kulish V. V., Malyi O. I., Persson C. and Wu P., *Phys. Chem. Chem. Phys.*, **17** (2015) 992.

[46] Kiraly B., Hauptmann N., Rudenko A. N., Katsnelson M. I. and Khajetoorians A. A., *Nano. Lett.*, **17** (2017) 3607.

[47] Li L. L. and Peeters F. M., *Phys. Rev. B*, **97** (2018) 075414.

[48] Li L. L., Partoens B. and Peeters F. M., *Phys. Rev. B*, **97** (2018) 155424.

[49] Li L. L., Moldovan D., Xu W. and Peeters F. M., *Phys. Rev. B*, **96** (2017) 155425.

[50] Yuan S., van Veen E., Katsnelson M. I. and Roldan R., *Phys. Rev. B*, **93** (2016) 245433.

[51] Song C. and Wang P., *Rev. Sci. Instrum.*, **81** (2010) 054702.

[52] Zhang D., *et al.*, *Phys. Rev. Lett.*, **111** (2013) 156402.

[53] Miao M. S., *et al.*, *Phys. Rev. Lett.*, **109** (2012) 186803.